Title
Dynamic Graph Convolution Based on Functional Neuroimaging Priors for EEG Mental Fatigue Recognition on Cross-subject

Journal
Proceedings of the Annual Meeting of the Cognitive Science Society, 46(0)

Authors
Jiang, Man
Jin, Jianxiu
Huang, Xubin
et al.

Publication Date
2024

Dynamic Graph Convolution Based on Functional Neuroimaging Priors for EEG Mental Fatigue Recognition on Cross-subject

Man Jiang (202121013298@mail.scut.edu.cn)
School of Electronic and Information Engineering, South China University of Technology
Guangzhou, China

Jianxiu Jin* (jxjin@scut.edu.cn)
School of Electronic and Information Engineering, South China University of Technology
Guangzhou, China

Xubin Huang (huangxubin@gpdi.com)
Guangdong Telecom Planning and Design Institute Co., Ltd
Guangzhou, China

Zirui Xiang (202221012653@mail.scut.edu.cn)
School of Electronic and Information Engineering, South China University of Technology
Guangzhou, China

Lin Shu* (shul@scut.edu.cn)
School of Future Technology, South China University of Technology
Guangzhou, China

Abstract

Mental fatigue among drivers is a primary factor in many traffic accidents. Electroencephalography (EEG), which directly measures neurophysiological activities in the brain, is commonly used for fatigue recognition. However, cross-subject research in fatigue recognition using EEG faces challenges such as low spatial resolution and significant individual variability. Inspired by neuroscience, a dynamic graph convolution learning from functional neuroimaging (FNI-DGCNN) is proposed, making up for EEG's low spatial resolution. We first use a multi-scale spatiotemporal learning block to extract EEG features with attention allocation, then initialize the adjacency matrix based on prior knowledge about fatigue recognition mechanisms from functional neuroimaging, use the extracted features and the adjacency matrix to initialize the graph, and finally use dynamic graph convolution further to study the intrinsic functional connectivity of mental fatigue. The proposed method achieves an accuracy of 88.89% among 17 subjects, outperforming existing EEG models for cross-subject.

Keywords: EEG; fatigue recognition; cross-subject; graph neural network; functional neuroimaging priors

Introduction

Mental fatigue, stemming from excessive brain activity, manifests as reduced alertness and attentional lapses. It is particularly perilous in professions that require extended periods of focused attention, such as pilots and drivers. Electroencephalography (EEG), which directly captures the brain's neurophysiological activities, has been widely used to identify mental fatigue recently (Budak et al., 2019; Sarailoo et al., 2022; Wang et al., 2023).

Several studies used manually extracted features to decode EEG signals based on machine learning algorithms. Rohit et al. (2019) used power spectral density features to predict driver fatigue. Min et al. (2021) used a hybrid model to obtain fatigue prediction results from the forehead EEG entropy features. Compared to machine learning methods, convolutional neural network (CNN) methods have shown competitive results for fatigue recognition. In the work of Gao et al. (2019), an EEG-based spatiotemporal convolutional neural network (ESTCNN) is developed for fatigue recognition. Chen et al. (2022) used a CNN model to extract hidden features from the adjacency matrix with a phase lag index (PLI). However, typical CNN-based methods are more suitable for processing regular and ordered Euclidean data, while the location of brains regions is in non-Euclidean space. For different tasks, there are distinct functional connectivity networks between brain regions (Lynch et al., 2018). Processing EEG through CNN cannot thoroughly learn the interconnections between multi-channel EEG signals.

Recently, graph convolutional neural network (GCNN) combines CNN with spectral theory (Defferrard, Bresson, & Vandergheynst, 2016), showing superiority in processing graph data. GCNN provides an efficacious method for exploring the intrinsic relationships of different graph nodes and analyzing multi-channel EEG. Song et al. (2020) proposed a DGCNN network by introducing the GCNN into EEG-based emotion recognition. Another work proposed a regularized graph neural network (RGNN) and performed well on emotion recognition (Zhong, Wang, & Miao, 2020).

In L. K. Samuelson, S. L. Frank, M. Toneva, A. Mackey, & E. Hazeltine (Eds.), *Proceedings of the 46th Annual Conference of the Cognitive Science Society.*

Wang et al. applied graph attention network (GAT) to fatigue recognition (2021) and overperformed compared models.

Although GCNN provides an efficacious method, EEG is still challenging in cross-subject research due to low spatial resolution and obvious individual differences. Sohrabpour et al. (2016) used Electromagnetic source imaging (ESI) to identify network nodes from EEG/Magnetoencephalography (MEG) and extracted time courses to construct directional functional connections of cortex brain networks. However, ESI can only achieve good results at high-density (⩾64 channels) scalp EEG (Seeber et al., 2019; Sohrabpour et al., 2015), while many published datasets have less than 64 EEG channels (Cao et al., 2019; Luo et al., 2019; Zheng & Lu, 2017).

Inspired by neuroscience, we propose a dynamic graph convolution learning from functional neuroimaging (FNI-DGCNN) to compensate for EEG's low spatial resolution and make it better suited for cross-subject research. A multi-scale spatiotemporal learning block is used to extract EEG features with attention allocation. The adjacency matrix is initialized based on prior knowledge about fatigue from functional neuroimaging. Finally, DGCNN is used further to study the intrinsic functional connectivity of mental fatigue.

Methods

In this section, the dataset description and processing are first introduced. Then, FNI-DGCNN and related basic works are introduced.

Dataset Description and Processing

Dataset To study the mental fatigue of cross-subject, experiments are conducted on a publicly available sustained-attention driving task dataset (Cao et al., 2019). 27 subjects participated in a 90-minute sustained-attention driving simulation to induce fatigue. During the task, lane departure events were randomly triggered, causing the car to drift to the cruising both sides from the lane (deviation onset). Each subject was expected to respond quickly by turning the wheel (response onset) to move the car back to the original lane (response offset). The next event occurred within 5–10 seconds after the current was completed. The reaction time to sudden events could objectively reflect the subject's fatigue.

EEG signals were recorded through a wired cap at a sampling rate of 500Hz with 32 Ag/AgCl electrodes placed based on a modified international 10-20 system, including 30 valid channels and 2 reference channels.

The raw data were bandpass filtered from 1-50Hz. The dataset authors performed initial manual removal of eye blink contamination, followed by applying Automatic Artifact Removal (AAR) techniques to correct ocular and muscular artifacts.

Data preparation The processed data are down-sampled to 250 Hz in our work. The EEG segments from 3 seconds before to 2 seconds after the deviation onset of each trial are extracted as the epoch, as shown in Figure 1. Fatigue levels are defined by reaction time (RT). Specifically, local RT measures the time from deviation onset to response onset as a marker of short-term fatigue level. Moreover, the average of local RTs across all epochs within the 90 seconds preceding the current epoch is defined as global RT, representing long-term fatigue level. The 5th percentile of all local RTs during the driving task is alert RT. Afterward, epochs with global RT and local RT less than 1.5 times alert RT are labeled as “Awake,” while both more significant than 2.5 times alert RT are labeled as “Fatigue.” With such classification, transition trials corresponding to moderate driver performance are excluded, which could benefit the accuracy of fatigue recognition (Wei et al., 2015). 3762 “Awake” epochs and 2794 “Fatigue” epochs from 17 subjects are extracted. Other subjects are excluded due to an imbalance in the positive and negative sample ratio (1:5).

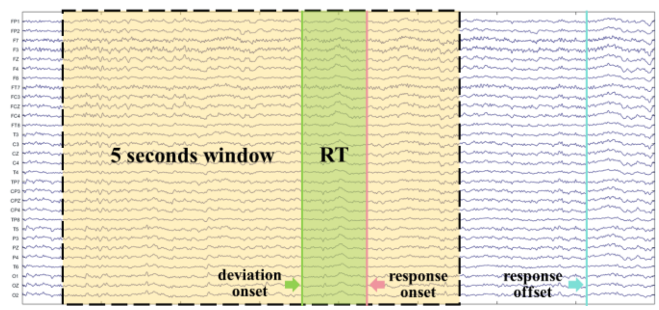

Figure 1: Epochs extraction.

FNI-DGCNN

The framework of FNI-DGCNN is shown in Figure 2, concluding with a spatiotemporal learning block to extract EEG features with attention allocation, a functional neuroimaging learning block to initialize the adjacency matrix, and a dynamic graph learning block to analyze the intrinsic functional connectivity associated with mental fatigue adaptively.

Spatiotemporal Learning Block There are two modules in this block: the temporal convolution layers and the temporal-spatial attention layers, as shown in Figure 2(a).

In the temporal convolution layer, the dilated convolution is used to learn new feature representations for each channel, which has a wider receptive field than standard convolution (Yu, Koltun & Funkhouser, 2017). Specifically, there are three dilated convolution layers with a (1, 3) kernel size, a (1, 2) stride, and dilation rates set at 1, 2, and 5, enabling the learning of multi-scale temporal features. Following each convolution layer are batch normalization, a leaky rectified linear unit (LeakyReLU), and a temporal-spatial attention layer for attention allocation learning.

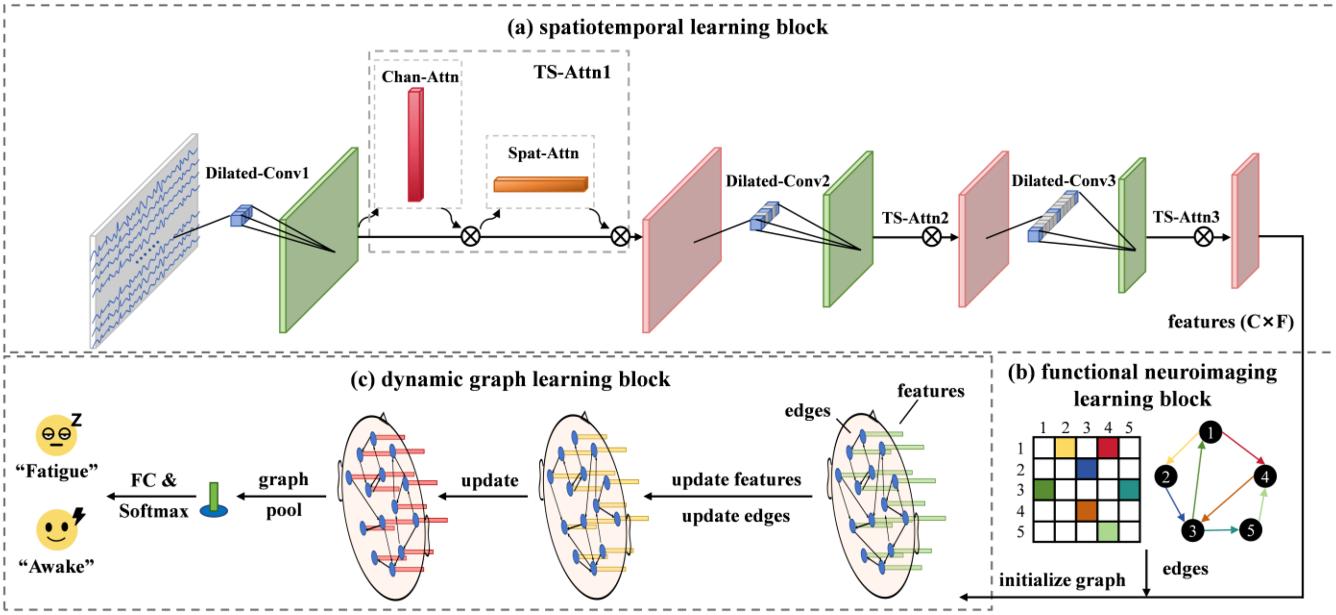

Figure 2: The framework of FNI-DGCNN. (a) spatiotemporal learning block; (b) functional neuroimaging learning block; (c) dynamic graph learning block.

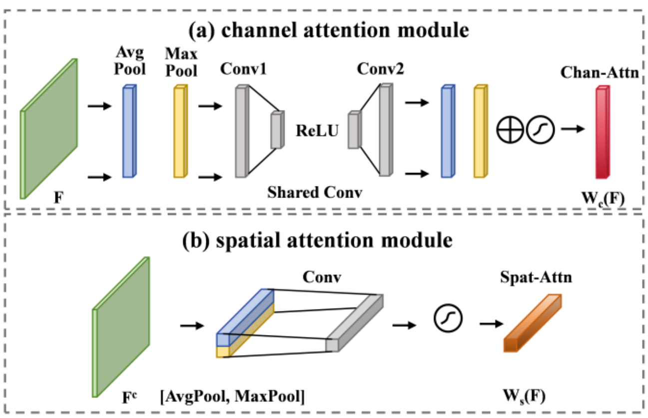

Figure 3: (a) channel attention module; (b) spatial attention module.

The temporal-spatial attention layer is improved based on the convolutional block attention module (CBAM) (Woo et al., 2018) to adapt to EEG signals. It consists of a channel and a spatial attention module. As depicted in Figure 3(a), the channel attention module uses average and maximum pooling to aggregate feature information in the time dimension for each input EEG channel data and then pass through a shared convolution network, respectively. Specifically, they are sequentially reduced in dimension by a CNN layer, activated by the ReLU function, and raised in dimension by a CNN layer to the same number of EEG channels. Finally, add them and activate using the sigmoid function to get channel attention weight $W_c(\mathrm{F})$. The feature map F passing through the channel attention layer can be calculated as

$$F^c = F \otimes W_c(\mathrm{F}) \tag{1}$$

where ⊗ denotes element-wise multiplication.

As shown in Figure 3(b), the spatial attention module uses average and maximum pooling to aggregate feature information in the channel dimension, respectively. The results are concatenated and reduced to 1 dimension by a CNN layer, then activated by the sigmoid function to get spatial attention weight $W_s(F^c)$. The feature map F^c passing through the spatial attention layer can be calculated as

$$F^s = F^c \otimes W_s(\mathrm{F}^c) \tag{2}$$

Functional Neuroimaging Learning Block To compensate for EEG's low spatial resolution, we propose a method for constructing an EEG-based functional connection network (FCN) from functional neuroimaging priors.

A review summarized what was learned from functional neuroimaging about the cortical core network of mental fatigue (Langner & Eickhoff, 2013). It encompasses the anterior insula, dorsomedial, mid- and ventrolateral prefrontal cortex, parietal, and subcortical structures, as depicted in Figure 4(a). In our work, standard Montreal Neurological Institute (MNI) stereotactic coordinates are first obtained by mapping EEG electrodes to the cortex (Koessler et al., 2009; Okamoto et al., 2004). Next, the MNI coordinates are transformed into Talairach space by icbm2tal transformation. Then, the brain regions corresponding to the EEG electrodes are analyzed using the Talairach client. Finally, the electrodes are matched to the core cortex nodes in Figure 4(a) based on the analysis, and the EEG-based FCN (total 317 edges) of mental fatigue is constructed.

To set up the adjacency matrix $\boldsymbol{W}$, we first calculate the distance $dist_{ij}$ between electrodes through MNI coordinates

$$dist_{ij} = \sqrt{(x_i - x_j)^2 + (y_i - y_j)^2 + (z_i - z_j)^2} \quad (3)$$

where $i, j \epsilon [0, n]$, n represents the total number of electrodes.

And initialize $\boldsymbol{W}$ as

$$w_{ij} = \begin{cases} 0, & [\mathrm{i,j}] \notin \mathrm{FCN} \\ \exp\left(-\frac{[dist_{ij}]^2}{2\tau^2}\right), & [\mathrm{i,j}] \in \mathrm{FCN} \end{cases} \quad (4)$$

where τ is the 30th percentile of $dist_{ij}$ to map w_{ij} in [0, 1]. Additionally, edges not in the FCN will be set to 0 to incorporate functional neuroimaging prior knowledge.

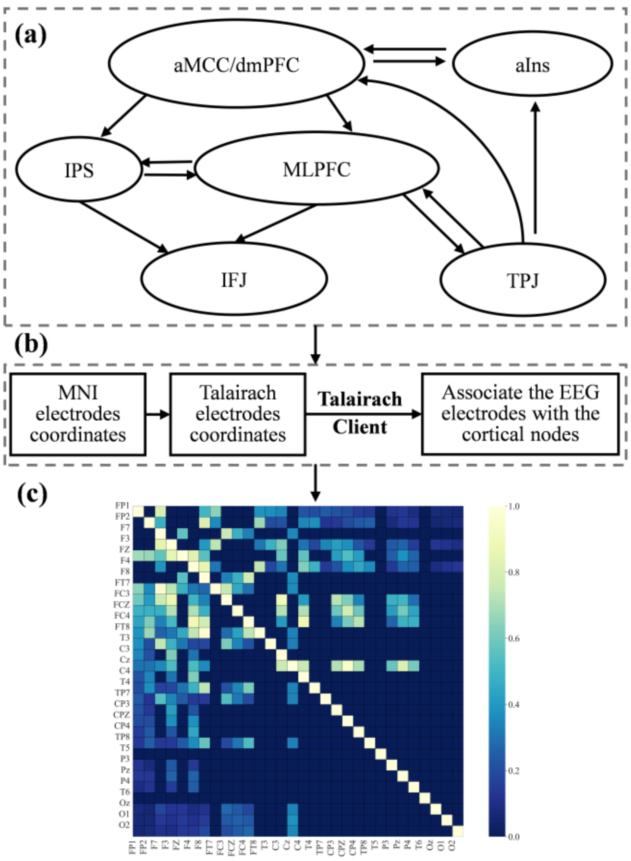

Figure 4: (a) Cerebral cortex core network: aMCC/dmPFC = anterior midcingulate cortex/dorsomedial prefrontal cortex; aIns = anterior insula; IPS = intraparietal sulcus; IFJ = inferior frontal junction; TPJ = temporoparietal junction; MLPFC = midlateral prefrontal cortex; (b) associating the EEG electrodes with the cortical nodes; (c) EEG-based FCN (total 317 edges) of mental fatigue.

Dynamic Graph Learning Block In this block, we extend DGCNN to learn the intrinsic functional connectivity associated with mental fatigue adaptively. The graph of EEG is denoted as $\boldsymbol{G} = \{\boldsymbol{V}, \boldsymbol{W}\}$, in which $\boldsymbol{V} = \{\boldsymbol{v_1}, \boldsymbol{v_2}, \cdots, \boldsymbol{v_n}\}$ is the vertex set with EEG electrodes, $\boldsymbol{W}$ is the adjacent matrix, and $\boldsymbol{w_{ij}}$ is the edge weight between $\boldsymbol{v_i}, \boldsymbol{v_j}$. Different from the DGCNN model, $\boldsymbol{W}$ is initialized in the FNI-DGCNN model by Eq. (4) to incorporate the mechanisms of mental fatigue faculty from functional neuroimaging.

Spectral graph theory extends convolution to the graph spectral domain. The Laplacian matrix L is expressed as $L = D - W$, where D is a $\mathbb{R}^{N \times N}$ diagonal matrix, $D_{ii} = \sum_{i=1}^{n} w_{ij}$. The Fourier basis U of G is an orthonormal matrix obtained from $L = U \Lambda U^T$, where Λ is a diagonal matrix obtained from $\Lambda = diag([\lambda_1, \lambda_2, \cdots, \lambda_n])$. Then, the graph convolution operator is defined as

$$x * y = U\big((U^T x) \odot (U^T y)\big) \quad (5)$$

where $\odot$ is Hadamard products. A signal x filtered by the filtering function $g(L)$ can be calculated as

$$y = g(L)x = g(U \Lambda U^T)x = U g(\Lambda) U^T x = x * (U^T x) \quad (6)$$

where $g(L)$ is designed as

$$g(\Lambda) = diag([\theta_1, \theta_2, \cdots, \theta_n]) \quad (7)$$

where θ_i is Fourier coefficient.

The graph layer of this paper is based on the simple graph convolution network (SGC) (Wu et al., 2019). The feature transformation between adjacent layers in GCNN can be expressed as

$$H^{l+1} = \sigma(W H^l \Theta^l) \quad (8)$$

where $l \in [0, L-1]$, L is the number of graph layers, Θ^l represents a weight matrix of layer l and σ is a non-linear function. To prevent H from growing to large, the feature transformation in graph convolution network (GCN) (Kipf & Welling, 2016) is improved as

$$H^{l+1} = \sigma(D^{-\frac{1}{2}} W D^{-\frac{1}{2}} H^l \Theta^l) \quad (9)$$

And SGC is proposed to further accelerate training by removing σ. And the output of SGC is expressed as

$$H^L = D^{-\frac{1}{2}} W D^{-\frac{1}{2}} H^{L-1} \Theta^{L-1} = S H^{L-1} \Theta^{L-1} = \cdots = S^L X \Theta \quad (10)$$

where $\Theta = \Theta^0 \Theta^1 \cdots \Theta^{L-1}$.

Features for each node are learned through two SGC layers. Subsequently, a global add graph pooling layer aggregates features over nodes. A dropout layer is then integrated to improve model generalization. The architecture is finalized with a fully connected layer and a softmax layer employed to classify fatigue levels. The class prediction $\hat{y}$ is obtained as

$$\hat{y} = softmax(pool(H^L)\Theta') \quad (11)$$

where Θ' is the weight transforming the SGC layer to the output layer.

Algorithm for FNI-DGCNN In addition to optimizing the network parameters $\boldsymbol{\Theta}$, $\boldsymbol{W}$ is also optimized to dynamically learn the intrinsic functional connectivity of mental fatigue.

The loss function is as followed

$$Loss = cross\_entropy(y, y^p) + \alpha\|W\|_1 + \beta\|\Theta\|_2 \quad (12)$$

where y, y^p denote the ground truth labels and predicted labels, α, β denote regularization weights and $\|\cdot\|_1, \|\cdot\|_2$ denote L_1, L_2 norm.

Results And Discussion

In this section, to evaluate the cross-subject effectiveness of the FIN-DGCNN model, we use the leave-one-subject-out (LOSO) cross-validation strategy to evaluate the overall performance and compare it with SVM, GAT, DGCNN, RGNN, Graph-U-Nets (Gao & Ji, 2022) and LGGNet (Ding et al., 2023) to explore the benefits of FIN-DGCNN further. Ablation studies are also conducted to analyze the impact of specific components.

Training is capped at 100 epochs with early stopping to minimize duration and prevent overfitting. The hidden size of SGC is 800. The dropout rate and batch size of all experiments are 0.5 and 256. We use Adam with an adaptive learning rate initialized as 0.01 to optimize model parameters. The regularization factors are both set as 0.003.

Methods Comparison

FIN-DGCNN is compared with SVM, GAT, DGCNN, RGNN, Graph-U-Nets, and LGGNet to explore the benefits of it further. Specifically, the SVM is adopted with five frequency bands differential entropy (DE) as inputs. For GAT, DGCNN, RGNN, and Graph-U-Nets, the spatiotemporal learning block is also used to extract features before the graph layer to give the model end-to-end capabilities. The ablation studies will explore the benefits of the spatiotemporal learning block. The adjacency matrices of GAT, DGCNN, and RGNN are adopted as the authors suggested. For Graph-U-Nets, the adjacency matrices adopted commonly used methods of phase locking value.

Table 1: Comparisons of average and standard deviations of ACC and F1 scores using seven classifiers.

Classifier	ACC (%)	F1 (%)
SVM	78.01/11.48	77.90/11.49
GAT	86.90/5.63	86.77/5.66
RGNN	85.47/7.17	85.44/7.07
DGCNN	87.52/6.03	87.32/6.11
Graph-U-Nets	87.75/5.68	87.40/6.10
LGGNet	86.17/9.93	86.26/9.56
FIN-DGCNN	**88.89/5.36**	**88.51/5.79**

The average and standard deviations of accuracies (ACC) and F1 scores are in Table 1 and Figure 5. The model proposed performs well on the public dataset; the evaluation metrics ACC and F1 scores are 88.89±5.36% and 88.51±5.79%, respectively. It is encouraging that FIN-DGCNN achieves better performance than all compared models. It performs ACC 10.88% better than the SVM model, which is attributed to the spatiotemporal learning block and the graph layers. In particular, our model performs better than other graph models, GAT, RGNN, DGCNN, Graph-U-Nets, and LGGNet, with the average ACC outperforming 1.99%, 3.42%, 1.37%, 1.14%, and 2.72%, the F1 score outperforming 1.74%, 3.07%, 1.19%, 1.11%, and 2.25%, respectively. The main improvement can be ascribed to the functional neuroimaging learning block, which initializes the adjacency matrix by incorporating the mechanisms of mental fatigue so that the model can learn the intrinsic connectivity of various brain regions regarding fatigue more effectively.

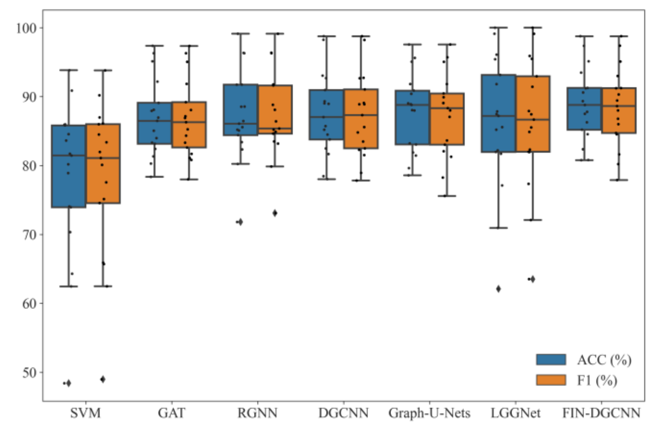

Figure 5: Comparisons of ACC and F1 scores using seven classifiers.

Ablation Study

The contribution of each block is assessed through ablation studies, where blocks are individually removed from the FIN-DGCNN model. Table 2 and Figure 6 report the recognition results on the public dataset.

We compare the model without the spatiotemporal learning block (− ST), replacing it with DE from five frequency bands. It is shown in Table 2 and Figure 6 that the FIN-DGCNN model outperforms "-ST" model by 8.5% with ACC and 7.39% with F1scores. The reason is that manually extracted features cannot capture higher-level abstract features during the training process, resulting in unsatisfactory performance. To further study, models without attention layers (− attention) and dilated convolution (− dilation) are compared, decreasing by 1.94% and 1.59% with ACC, 1.66%, and 1.28% with F1scores. It is explained that the attention block introduced can effectively extract features with attention allocation about the mechanisms of mental fatigue, and the dilated convolution can increase the receptive field and extract multi-scale features. Significantly, the attention layer only introduces very few increases in parameters, and the dilated convolution layer operates with fewer parameters than standard convolution.

The DGCNN model initialized the adjacency matrix only depending on the Euclidean Distance of EEG electrodes. Due to the volume conduction effect of EEG, the initialization method of DGCNN may introduce some false ingredients and limit the generalization ability in cross-subject study. Thus, compared with our method incorporating the mechanisms of mental fatigue faculty of functional neuroimaging prior knowledge, the DGCNN (− FNI) shows poor performance.

Table 2: The average and standard deviations of ACC and F1 scores. The symbol "−" indicates the following component is removed.

Classifier	ACC (%)	F1 (%)
FIN-DGCNN	**88.89/5.36**	**88.51/5.79**
− ST	80.39/10.73	81.12/9.97
− attention	86.95/5.84	86.85/5.79
− dilation	87.30/5.41	87.23/5.37
− FNI	87.52/6.03	87.32/6.11

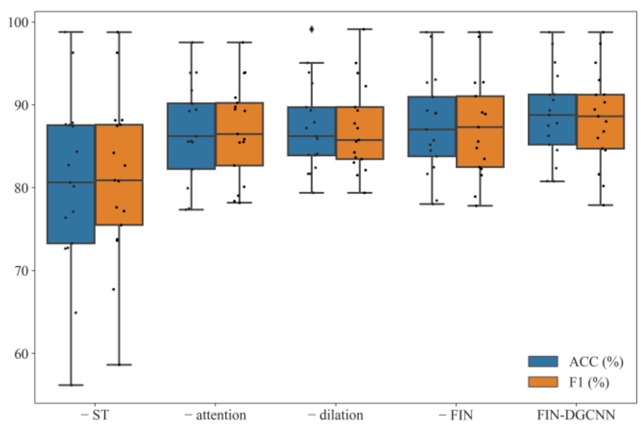

Figure 6: Comparisons of ACC and F1 scores of ablation studies.

To further analyze mental fatigue's EEG-based intrinsic functional connectivity, we visualize the initialization adjacency matrix and the final matrix learned from the FIN-DGCNN model, as shown in Figure 7. Specifically, the final matrix is obtained by summing all matrices of 17 subjects, mapping between 0 and 1, and showing the top 35% (total 315 edges).

There are 287 identical edges (91%) in the initial and final adjacency matrices, further demonstrating the effectiveness of the proposed functional neuroimaging learning block. Moreover, for the top 10% of edges, there are 78 identical edges (86.7%), including self-connections of all nodes. Among them, F3, F4, CP4, O2, O1, P3, Pz, CP3, Oz, and CPz show strong self-connections in sequence, mainly concentrated in the frontal, occipital, and parietal lobes. In addition, C4 to F4, F7 to FC3, F8 to FC4, F3 toFT7, C3 to F3, F3 to F7, Cz to CPz, and F7 to Fz also show strong connections in sequence, mainly concentrated in the frontal to frontal, central to frontal and central to parietal. The frontal lobes are associated with motor control, and the parietal and occipital lobes are associated with visual processing. Their strong self-connections may be attributed to the motor and visual processes of the fatigue driving task. The central is responsible for integrating information in the brain, which may explain its strong connections to the frontal and parietal lobes.

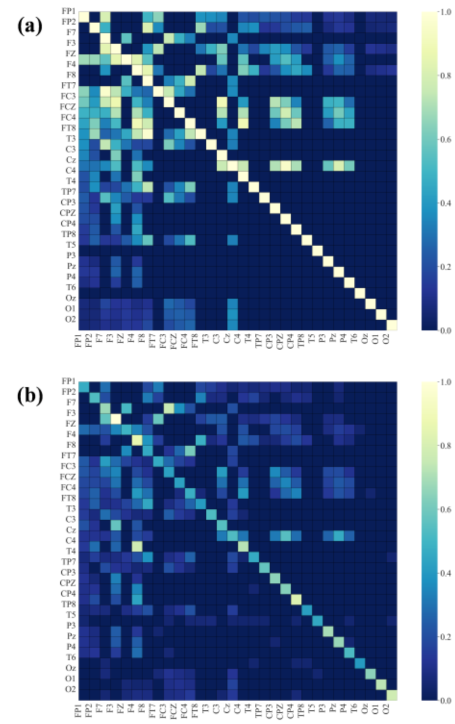

Figure 7: The adjacency matrix: (a) initialization; (b) final.

Conclusion

In this work, the FIN-DGCNN model for EEG-based mental fatigue recognition is proposed. The model is neurologically inspired to learn from the mechanisms of mental fatigue faculty of functional neuroimaging and study the intrinsic functional connectivity of EEG. A multi-scale spatiotemporal learning block to extract EEG features with attention allocation. Combined with functional neuroimaging research, a functional connectivity network of the mental fatigue mechanism is constructed to compensate for EEG's lack of spatial resolution. Then, the graph convolution is used to learn the intrinsic connectivity of mental fatigue dynamically. The proposed method achieves a cross-subject accuracy of 88.89% on a public drive fatigue dataset, outperforming five existing graph convolutional networks for EEG. The proposed method to apply functional neuroimaging prior knowledge to constructing the EEG-based graph performs well on fatigue recognition. In the future, it is expected to improve the model generalization ability in other specific tasks, such as motor imagery and emotion recognition.

Acknowledgments

This work is funded by Guangzhou Science and Technology Plan Project: High-Level Enterprise Research Institute Independently Selected Project Topic(202205110004).

References

Bose, R., Wang, H., Dragomir, A., Thakor, N. V., Bezerianos, A., & Li, J. (2019). Regression-based continuous driving fatigue estimation: Toward practical implementation. *IEEE Transactions on Cognitive and Developmental Systems, 12*(2), 323-331.

Budak, U., Bajaj, V., Akbulut, Y., Atila, O., & Sengur, A. (2019). An effective hybrid model for EEG-based drowsiness detection. *IEEE sensors journal, 19*(17), 7624-7631.

Cao, Z., Chuang, C. H., King, J. K., & Lin, C. T. (2019). Multi-channel EEG recordings during a sustained-attention driving task. *Scientific data, 6*(1), 19.

Chen, J., Wang, S., He, E., Wang, H., & Wang, L. (2022). Two-dimensional phase lag index image representation of electroencephalography for automated recognition of driver fatigue using convolutional neural network. *Expert Systems with Applications, 191,* 116339.

Defferrard, M., Bresson, X., & Vandergheynst, P. (2016). Convolutional neural networks on graphs with fast localized spectral filtering. *Advances in neural information processing systems, 29*.

Ding, Y., Robinson, N., Tong, C., Zeng, Q., & Guan, C. (2023). LGGNet: Learning from local-global-graph representations for brain–computer interface. *IEEE Transactions on Neural Networks and Learning Systems*.

Gao, H., & Ji, S. (2022). Graph U-Nets. *IEEE Transactions on Pattern Analysis & Machine Intelligence, 44*(09), 4948-4960.

Gao, Z., Wang, X., Yang, Y., Mu, C., Cai, Q., Dang, W., & Zuo, S. (2019). EEG-based spatio–temporal convolutional neural network for driver fatigue evaluation. *IEEE transactions on neural networks and learning systems, 30*(9), 2755-2763.

Kipf, T. N., & Welling, M. (2016, November). Semi-Supervised Classification with Graph Convolutional Networks. *In International Conference on Learning Representations*.

Koessler, L., Maillard, L., Benhadid, A., Vignal, J. P., Felblinger, J., Vespignani, H., & Braun, M. (2009). Automated cortical projection of EEG sensors: anatomical correlation via the international 10–10 system. *Neuroimage, 46*(1), 64-72.

Langner, R., & Eickhoff, S. B. (2013). Sustaining attention to simple tasks: a meta-analytic review of the neural mechanisms of vigilant attention. *Psychological bulletin, 139*(4), 870.

Luo, H., Qiu, T., Liu, C., & Huang, P. (2019). Research on fatigue driving detection using forehead EEG based on adaptive multi-scale entropy. *Biomedical Signal Processing and Control, 51*, 50-58.

Lynch, L. K., Lu, K. H., Wen, H., Zhang, Y., Saykin, A. J., & Liu, Z. (2018). Task-evoked functional connectivity does not explain functional connectivity differences between rest and task conditions. *Human brain mapping, 39*(12), 4939-4948.

Min, J., Xiong, C., Zhang, Y., & Cai, M. (2021). Driver fatigue detection based on prefrontal EEG using multi-entropy measures and hybrid model. *Biomedical Signal Processing and Control, 69*, 102857.

Okamoto, M., Dan, H., Sakamoto, K., Takeo, K., Shimizu, K., Kohno, S., ... & Dan, I. (2004). Three-dimensional probabilistic anatomical cranio-cerebral correlation via the international 10–20 system oriented for transcranial functional brain mapping. *Neuroimage, 21*(1), 99-111.

Sarailoo, R., Latifzadeh, K., Amiri, S. H., Bosaghzadeh, A., & Ebrahimpour, R. (2022). Assessment of instantaneous cognitive load imposed by educational multimedia using electroencephalography signals. *Frontiers in Neuroscience, 16*, 744737.

Seeber, M., Cantonas, L. M., Hoevels, M., Sesia, T., Visser-Vandewalle, V., & Michel, C. M. (2019). Subcortical electrophysiological activity is detectable with high-density EEG source imaging. *Nature communications, 10*(1), 753.

Sohrabpour, A., Lu, Y., Kankirawatana, P., Blount, J., Kim, H., & He, B. (2015). Effect of EEG electrode number on epileptic source localization in pediatric patients. *Clinical Neurophysiology, 126*(3), 472-480.

Sohrabpour, A., Ye, S., Worrell, G. A., Zhang, W., & He, B. (2016). Noninvasive electromagnetic source imaging and granger causality analysis: an electrophysiological connectome (eConnectome) approach. *IEEE Transactions on Biomedical Engineering, 63*(12), 2474-2487.

Song, T., Zheng, W., Song, P., & Cui, Z. (2020). EEG Emotion Recognition Using Dynamical Graph Convolutional Neural Networks. *IEEE Transactions on Affective Computing, 11*(3), 532-541.

Wang, Y., Huang, Y., Gu, B., Cao, S., & Fang, D. (2023). Identifying mental fatigue of construction workers using EEG and deep learning. *Automation in Construction, 151*, 104887.

Wang, Z., Zhao, Y., He, Y., & Zhang, J. (2021). Phase lag index-based graph attention networks for detecting driving fatigue. *Review of Scientific Instruments, 92*(9).

Wei, C. S., Wang, Y. T., Lin, C. T., & Jung, T. P. (2015, August). Toward non-hair-bearing brain-computer interfaces for neurocognitive lapse detection. In *2015 37th Annual International Conference of the IEEE Engineering in Medicine and Biology Society (EMBC)* (pp. 6638-6641).

Woo, S., Park, J., Lee, J. Y., & Kweon, I. S. (2018). Cbam: Convolutional block attention module. In *Proceedings of the European conference on computer vision (ECCV)* (pp. 3-19).

Wu, F., Souza, A., Zhang, T., Fifty, C., Yu, T., & Weinberger, K. (2019, May). Simplifying graph convolutional networks. *In International conference on machine learning* (pp. 6861-6871). PMLR.

Yu, F., Koltun, V., & Funkhouser, T. (2017). Dilated residual networks. *In Proceedings of the IEEE conference on computer vision and pattern recognition* (pp. 472-480).

Zheng, W. L., & Lu, B. L. (2017). A multimodal approach to estimating vigilance using EEG and forehead EOG. *Journal of neural engineering, 14*(2), 026017.

Zhong, P., Wang, D., & Miao, C. (2020). EEG-based emotion recognition using regularized graph neural networks. *IEEE Transactions on Affective Computing, 13*(3), 1290-1301.